Structural Eng. / Earthquake Eng. Vol. 7. No. 1, 133s-142s. April 1990
Japan Society of Civil Engineers (Proc. of JSCE No. 416/I-13)

MODIFIED DISTINCT ELEMENT METHOD SIMULATION OF DYNAMIC CLIFF COLLAPSE

By Kazuyoshi IWASHITA and Motohiko HAKUNO***

Usual Distinct Element Method (DEM), in which soil is represented as a system of numerous discrete particles, does not account for two factors ; the continuity of the medium and wave propagation. The modified method, which is proposed in this paper, has another physical structure which presents the effect of the internal material between particles as pore water or clay. We simulated the two dimensional dynamic fracture of a cliff using this method. The fracture process is as follows ; many small cracks occur widely then they form fracture lines. Results confirmed that this method can simulate the continuous and discontinuous medium.
Keywords : DEM, cliff collapse, dynamic fracture, continuity of the medium, fracture line

1. INTRODUCTION

Conventionally, the dynamic behavior of soil and of soil structures e. g. cliffs has been simulated by representing soil as continuous material, but another method has been developed in which soil is represented as discontinuous material[1),2)]. The conventional method simulated the process before fracture takes place, but it is difficult to use it to simulate the actual process of fracture. The newer method simulates the fracture process sequentially from the formation of small cracks to large slides. The DEM is one example of this new type of method. In the DEM, soil is represented as a system of numerous discrete particles, the dynamic behavior of each being calculated individually. This method is based on the concept that each particle satisfies the equation of motion and that particle interaction is simple. Recently the DEM has been used to investigate problems related to various phenomena ; rock systems (Cundall[1)]), tunnels (Kiyama *et al.*[3)]), gravity flow of granular particles (Kiyama and Fujimura[4)]) slope stability (Uemura and Hakuno[5)], Casaverde *et al.*[6)]) and the liquefaction process (Tarumi and Hakuno[7)]).

The DEM, however, does not account for two important factors ; the continuity of the medium and wave propagation. Equilibrium in DEM is unstable because, between particles there is compressive but no tensile force. Therefore, because of this lack of stability, DEM models cannot be used for free-surface problems. Many problems which are not solvable by the techniques of conventional continuous mechanics can, however, be investigated with this method. We here report an improved DEM which takes into account the continuity of the medium and wave propagation.

---

* Member of JSCE, Dr. Eng., Assistant Professor, Dept. of Foundation Eng., Saitama Univ. (Shimo-ohkubo 255, Urawa, Saitama 338)
** Member of JSCE, Dr. Eng., Professor, Earthquake Research Institute, University of Tokyo (Yayoi 1-1-1, Bunkyo-ku, Tokyo 113)

2. METHODS

The flow of the modified DEM program is shown in Fig. 1. DEM is an iterative calculation method in time domain, and the future state is calculated from the present stage. The particles in this new DEM have not been changed, but a mechanical structure has been added to introduce stable equilibrium. Therefore, there are two structures ; a primary and a secondary one (diagram Fig. 2). The primary structure consists of the conventional DEM and is used to transmit the force F_{s1} though the contact points between particles and to calculate particle movement. It deals with the rotation of particles, but does not function when particles are not in contact. It serves to conduct energy between two contacting particles. This structure has two components ; a normal and a tangential one. Each component has three elements ; an elastic spring, a viscous dashpot and a no tension joint. Formation of this primary structure is the same as in the conventional DEM.

The secondary structure represents stable equilibrium and shows the continuity of the medium. For example the first structure might correspond to rock or gravel and the second to internal clay or pore water. This structure is set between particles in contact and near particles as well. As Fig. 2, the secondary structure and masses make a mass-spring system, then it can represent the stable equilibrium and the continuity of the medium. It can transmit the wave propagation. And the secondary structure is destructible, then this system can represent the small cracks and the fracture process. The secondary structure has two components ; a normal and a tangential one. If the medium is a plastic one, the elements of each component will form a Voigt model that is a complex of an elastic spring and a viscous dashpot, or some other physical model. This structure does not take into account the effect of the rotation of particles. We used an elastic spring for simplicity. The neutral length of the spring is the distance between two particles in the initial condition. Therefore the reaction of the secondary structure, F_{s2}, moves the particles to the initial relative location. The secondary structure system tends to keep the particles in the initial location.

Fig. 3 is the force-displacement law of the secondary structure. The closeness of two particles, I and J, is found by

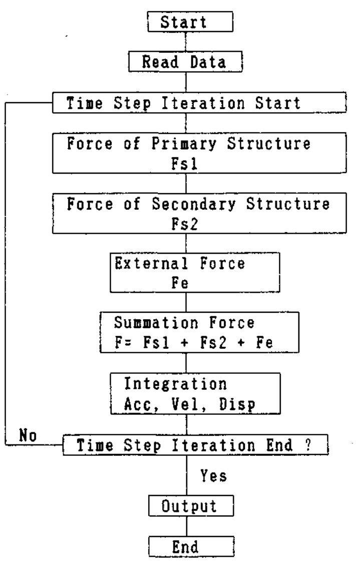

Fig. 1 Flow Chart of the Modified DEM.

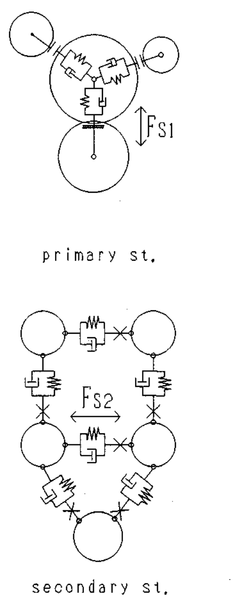

Fig. 2 Scheme of the Improved DEM (only plotting the normal component).

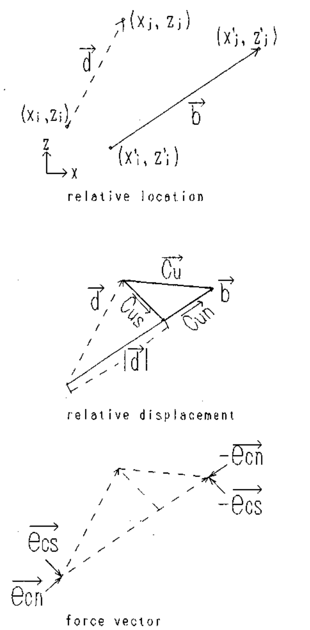

Fig. 3 Force-Displacement Law of the Secondary Structure.

$$(r_i+r_j)\times DCR\,1 \geqq R_{ij} \quad (1)$$

$$R_{ij}=\sqrt{(x_j-x_i)^2+(z_j-z_i)^2} \quad (2)$$

in which r_i and r_j are the radii of the particles ; (x_i, z_i) and (x_j, z_j) are the coordinates of the center ; and $DCR\,1$ is the coefficient of closeness. Usually, $DCR\,1$ is greater than 1.0. R_{ij} is the distance between the centers. The secondary structure is set up among particles that satisfy this condition.

The initial relative direction vector $\vec{d}$ is

$$\vec{d}=(x_j-x_i,\ z_j-z_i) \quad (3)$$

This vector shows the neutral direction of the secondary structure. At time t, the coordinates of I and J are (x'_i, z'_i) and (x'_j, z'_j). The relative direction vector $\vec{b}$ is

$$\vec{b}=(x'_j-x'_i,\ z'_j-z'_i) \quad (4)$$

The relative movement vector $\overrightarrow{C_u}$ from time 0 to t is

$$\overrightarrow{C_u}=\vec{b}-\vec{d} \quad (5)$$

$\overrightarrow{C_u}$ is analyzed in the local coordinates, the normal component $\overrightarrow{C_{un}}$ and the tangential component $\overrightarrow{C_{us}}$.

$$\overrightarrow{C_{un}}=(|\vec{b}|-|\vec{d}|)\times\vec{b}/|\vec{b}| \quad (6)$$

$$\overrightarrow{C_{us}}=\overrightarrow{C_u}-\overrightarrow{C_{un}} \quad (7)$$

The force vectors of the springs $\overrightarrow{e_{cn}}$ in the normal and $\overrightarrow{e_{cs}}$ in the tangential direction, are defined as

$$\overrightarrow{e_{cn}}=k_{cn}\cdot\overrightarrow{C_{un}} \quad (8)$$

$$\overrightarrow{e_{cs}}=k_{cs}\cdot\overrightarrow{C_{us}} \quad (9)$$

in which k_{cn} and k_{cs} are the spring constants.

The force F_{s2ij} which works from particle J to I by way of the secondary structure and $\overrightarrow{F_{s2ji}}$ which works from I to J are

$$\overrightarrow{F_{s2ij}}=-\overrightarrow{F_{s2ji}}=\overrightarrow{e_{cn}}+\overrightarrow{e_{cs}} \quad (10)$$

The force $\overrightarrow{F_{s2i}}$ which works at I in the secondary structure is

$$\overrightarrow{F_{s2i}}=\sum_j\overrightarrow{F_{s2ij}} \quad (11)$$

The total force $\overrightarrow{F_i}$ which works at I at time t is

$$\overrightarrow{F_i}=\overrightarrow{F_{s1i}}+\overrightarrow{F_{s2i}}+\overrightarrow{F_{ei}} \quad (12)$$

in which $\overrightarrow{F_{s1i}}$ is the total force at particle I produced by the primary structure and $\overrightarrow{F_{ei}}$ is the external force and gravity.

Particle I's acceleration, $\overrightarrow{A_{it}}$, at time t is

$$\overrightarrow{A_{it}}=\overrightarrow{F_i}/m_i \quad (13)$$

in which m_i is the mass of particle I.

The velocity and displacement at time $t+\Delta t$ is defined by integration with $\overrightarrow{A_{it}}$ and an increment of the time step iteration Δt. The state at time $t+2\,\Delta t$ can be calculated from the state at $t+\Delta t$ by iteration.

In the initial condition, the secondary structure is passive. The particles move because of the force of the primary structure, after which the secondary structure moves.

If the elements of the secondary structure receive critical strain, the structure will break and be partially unworkable. Tensile fracture in the normal direction due to strain is supposed, as **Fig.** 4 [A]. It occurs under the following condition,

$$|\vec{b}|\geqq|\vec{d}|\cdot DCR\,2 \quad (14)$$

in which $DCR\,2$ is the coefficient of the fracture strain.

Shear fracture in the tangential direction due to stress also is supposed, as **Fig.** 4 [B]. Coulomb's criterion is used. In the DEM scheme, force is used in place of stress ; thus the criterion is also represented in force.

$$|\overrightarrow{e_{cs}}|=C_{DEM}+|\overrightarrow{e_{cn}}|\times\tan\phi \quad (15)$$

in which C_{DEM} is the proportional cohesion c, and ϕ is the friction angle. Eq. (15) is used when particles are under compression. When the particles are under tension, no friction factor exists because there is no friction.

$$|\overrightarrow{e_{cs}}| = C_{DEM} \qquad (16)$$

Fracture in the shear and normal directions can be simulated in this way. When the destroyed part of the secondary structure does not work, the stress concentrates on the remaining active part and the fracture spreads. It is important to be able to express the fracture in the secondary structure. By plotting the active, but not the destroyed parts, of this structure, as **Fig. 10** the process of fracture can be expressed accurately.

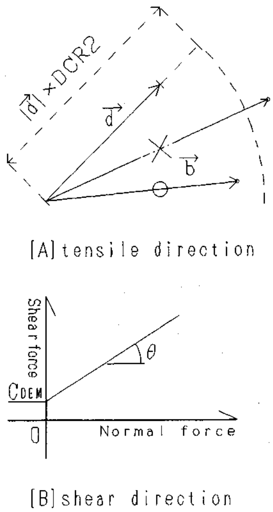

Fig. 4 Fracture Law of the Model (tensile [A] ; shear [B]).

3. DECISION OF PARAMETERS

Our new DEM model has double springs in both the normal and tangential directions. The spring constant of the primary structure represents the stiffness of the medium, and the constant of the secondary structure affects the elastic wave velocity. The former value is larger than the latter. Consequently, the total stiffness of the model is similar to that of the primary structure.

Same method can be used to define the parameters of the primary structure as Kiyama *et al.*.

The parameters of the secondary structure are defined by assuming the distinct element model as the continuous element model as **Fig. 5**.

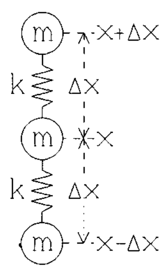

Fig. 5 One-Dimensional Mass-Spring System.

The equation of motion about 1 dimensional mass-spring system is

$$m\frac{\partial^2 y}{\partial t^2} = k(y_{x-\Delta x} - y_x) - k(y_x - y_{x+\Delta x}) = k(y_{x-\Delta x} - 2y_x + y_{x+\Delta x}) \qquad (17)$$

in which y is the displacement, m is mass and k is the spring constant.

The wave equation is

$$\frac{\partial^2 y}{\partial t^2} = V^2\frac{\partial^2 y}{\partial x^2} \qquad (18)$$

in which V is the wave velocity. The central difference equation is conducted from eq. (18).

$$\frac{\partial^2 y}{\partial x^2} \fallingdotseq \frac{1}{\Delta x^2}(y_{x-\Delta x} - 2y_x + y_{x+\Delta x}) \qquad (19)$$

in which Δx is the length of mesh.

From the eq. (18) and (19), following relationship is conducted.

$$\frac{\partial^2 y}{\partial t^2} = V^2\frac{\partial^2 y}{\partial x^2} = \frac{V^2}{\Delta x^2}(y_{x-\Delta x} - 2y_x + y_{x+\Delta x}) \qquad (20)$$

Relationship between V and the spring constant k is induced from eq. (17) and (20).

$$\frac{k}{m} = \frac{V^2}{\Delta x^2} \qquad (21)$$

In 2 dimensional DEM, m and Δx are

$$m = \pi r^2 \rho \qquad (22)$$

$$\Delta x = 2r \qquad (23)$$

in which ρ is density and r is the radius of the particle.

In normal direction between the particles, V and k correspond to V_P, primary wave velocity, and k_{cn}.

$$k_{cn} = \pi\rho V_P^2/4 \qquad (24)$$

In tangential direction, they correspond to V_S, secondary wave velocity, and k_{cs}.

$$k_{cs} = \pi\rho V_S^2/4 \qquad (25)$$

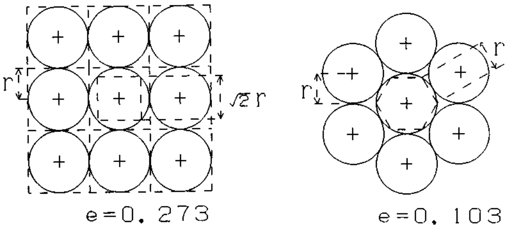

Fig. 6 The geometrical Disposition of the Particles.

Table 1 Parameters of the model.

No. of Particles	1000	
Radius max	15.0	(cm)
min	5.0	(cm)
mean	10.0	(cm)
σ	0.15	
Size Width	10	(m)
Height	3	(m)
k normal dir.	6.0×10^{6}	(N/m)
k tangential dir.	1.5×10^{6}	(N/m)
Viscous coefficient	0.0	(NSec/m)
ϕ	11	(°)
Restitution coefficient	0.2	
ρ	2000.0	(kg/m³)
Δt	0.001	(sec)
DCR1	1.2	
C_{DEM}	1000	(N)
k_{CN}	1.2×10^{6}	(N/m)
k_{CS}	1.0×10^{6}	(N/m)

ϕ is decided from a dynamic friction factor μ.

$$\phi=\arctan\mu \quad (26)$$

The dimension of C_{DEM} is force (N). Then C_{DEM} is

$$C_{DEM}=a\cdot C \quad (27)$$

in which a is the area of contact plane between the particles.

In this study we use a cylinder element, which length is unit length, for the particle. The contact plane between two cylinder is a square. Fig. 6 shows two geometrical disposition of the particles. The length of the one side of the inscribed regular polygon is suitable to the length of the one side of the contact square. Because as increasing the edges of the polygon, $\sum a$ and $\sum C_{DEM}$ increases and each a and C_{DEM} decrease.

The void ratio e of the case [A] is 0.273 and a is

$$a=\sqrt{2}\ r\times1 \quad (28)$$

The void ratio e of the case [B] is 0.103 and a is

$$a=r\times1 \quad (29)$$

a of the other disposition model can be decided in proportion to each e and C_{DEM} can be calculated.

4. TESTS

(1) Two-dimensional cliff model test

To test our modified DEM, we applied it to the dynamic fracture of a cliff caused by its mass and applied cyclic force. The two-dimensional cliff model used was 3×10 m². Table 1 shows the parameters for that model and our calculations. The number of particles was 1 000, particle radius being defined by Normal Random Distribution based on a maximum radius of 15 cm and a minimum radius of 5 cm. This ground was made very softly, V_P is about 30 m/sec and V_S is 10 m/sec, to decrease the CPU time. The applied force was a cyclic wave in the horizontal direction that was input from the bottom of the model. In another test, the slope was cut away from the cliff model and the remainder stabilized and used as a bank model.

The model was set in a square box with three walls, then at 0 sec the right wall having been eliminated.

a) Without a secondary structure or applied force

Use of the conventional DEM. (Fig. 7) showed particle movement and the distribution of velocity. The cliff disintegrated because of its mass. In this case, the model showed acute collapse and it was difficult to distinguish the destroyed from the stable area.

At early stage, the front of the cliff falls down and the shape of rockfall has roundness. Then the particles of inner part roll down the slope. At 4 sec, the slope angle of the rockfall is 15°. It is similar to

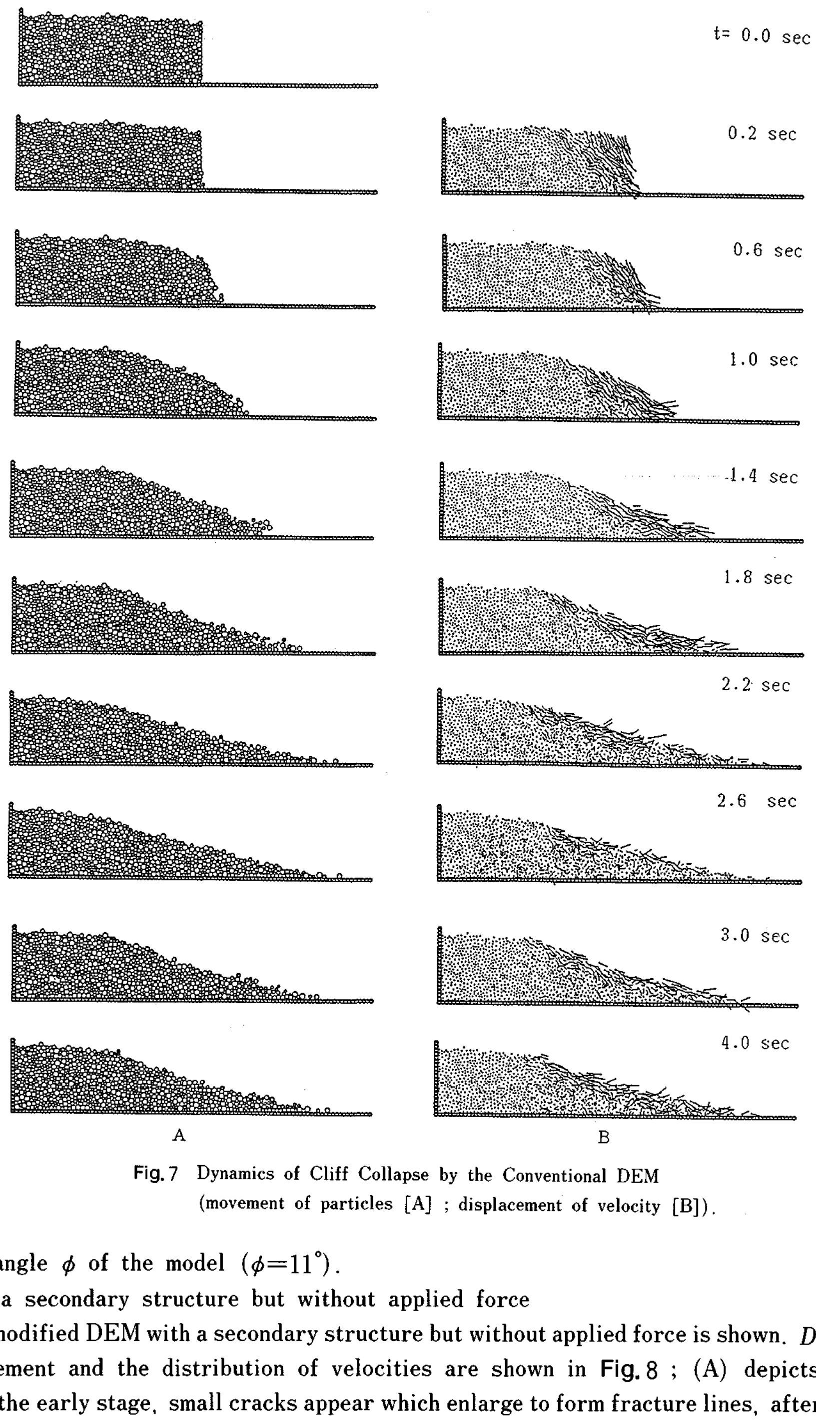

Fig. 7 Dynamics of Cliff Collapse by the Conventional DEM (movement of particles [A] ; displacement of velocity [B]).

the friction angle ϕ of the model ($\phi=11^\circ$).

b) With a secondary structure but without applied force

Use of the modified DEM with a secondary structure but without applied force is shown. $DCR\,2$ is 1.02. Particle movement and the distribution of velocities are shown in Fig. 8 ; (A) depicts the primary structure. In the early stage, small cracks appear which enlarge to form fracture lines, after which blocks of soil begin to slide.

Fig. 9 shows the growing of the small cracks at time 0.2, 0.4 and 1.0 sec. At early stage, the small cracks occur all over the front part of the cliff, then they connect and make a fracture line gradually. The most of the cracks occur due to tension and few cracks occur due to shear force. In this case, the fracture line seems to occur due to tension. At 4 sec, the angle of the rockfalls is also 15°.

c) With a secondary structure and an applied force

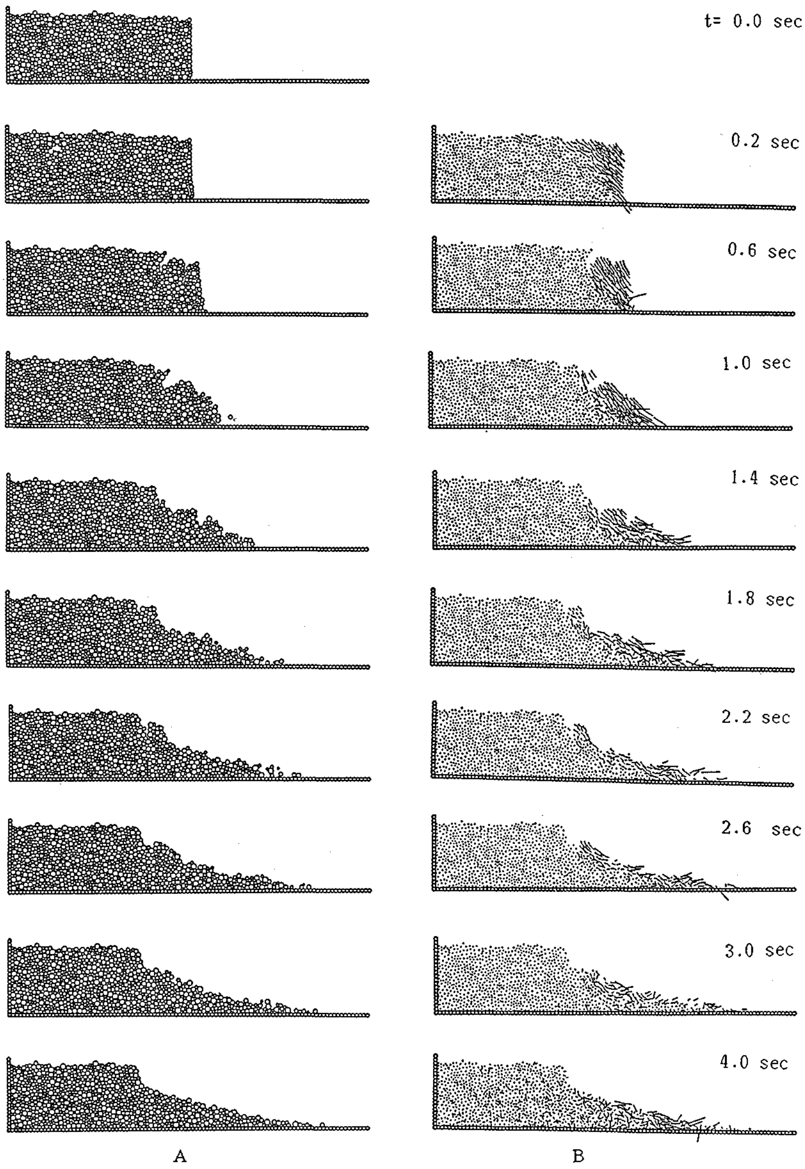

Fig. 8 Dynamics of Cliff Collapse by the Modified DEM (movement of particles [A] ; distribution of velocity [B]).

This case uses cyclic force to represent an earthquake. The amplitude of the applied acceleration is about 800 gal, and DCR 2 is 1.05. The primary and secondary structures of the cliff model at 0, 2 and 4 sec are shown in Fig. 10 [A] and [B]. The area that was erased at 2 sec and 4 sec in the secondary structure is the fracture in which the secondary structure is destroyed due to critical strain. The destroyed points are located linearly and they form the fracture lines. The secondary structure clearly shows the lengthening of cracks and sliding ; progressive sliding appears, the soil moving in blocks. The effects of having a secondary structure are shown in Fig. 11. Results for 3 cases are given ; without a secondary structure or an applied force ; with a secondary structure, but no applied force ; and with a secondary structure and an applied force. The original DEM does not distinguish the broken from the stable area. The angle of the rockfall is 15° in these three cases. This result shows that the slope angle is related to the friction angle ϕ

among the particles.

(2) Two-dimensional bank model test

The fracture processes for banks with slopes of 45° and 30° are shown in Figs. 12 and 13. The numbers of particles are 848 for the 45° slope and 712 for the 30° slope. The other parameters are the same as in Table 1. The 45° bank is soon broken. The secondary structure shows cracks formed perpendicular to the slope. Fracture lines are clear, and the bank slides along those lines. Many small cracks occur in the lower part of the bank model. Then they are connected, form a fracture line and extend to the upper. Finally the bank sinks and slides to the free side. By parameter study, it is found out that the model which is made from soft soil sinks deeper than hard one. These results are similar to observations of actual sliding caused by an earthquake.

5. CONCLUSIONS

The secondary structure of our modified DEM model and the particles make a mass-spring system, then the modified DEM can represent the stable equilibrium and the continuity of the medium.

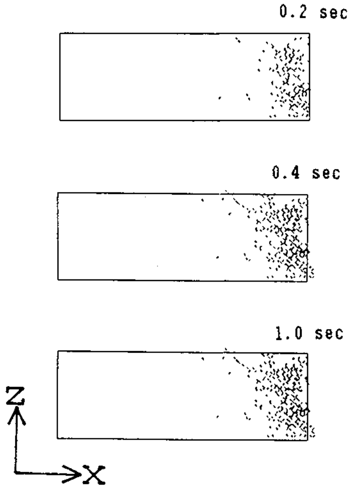

Fig. 9 The Distribution of the Cracks (bold lined cracks occur due to shear, thin lined cracks occur due to tension).

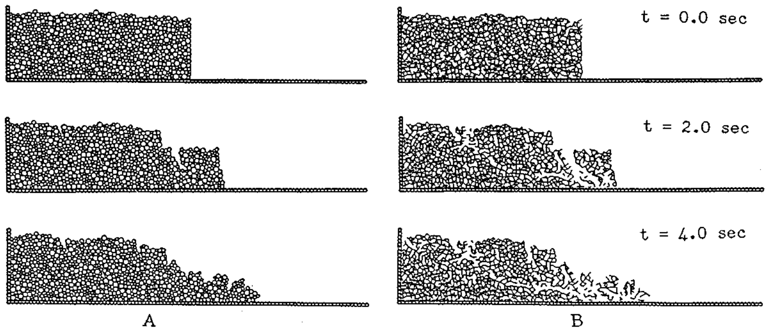

Fig. 10 The Primary [A] and Secondary [B] Structures of a Cliff.

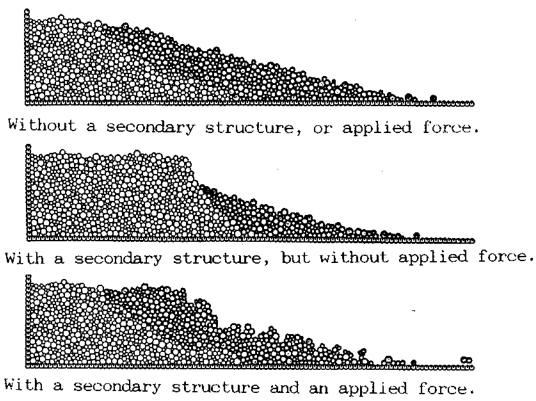

Fig. 11 Effects of the Secondary Structure (Shaded particles move from their initial positions).

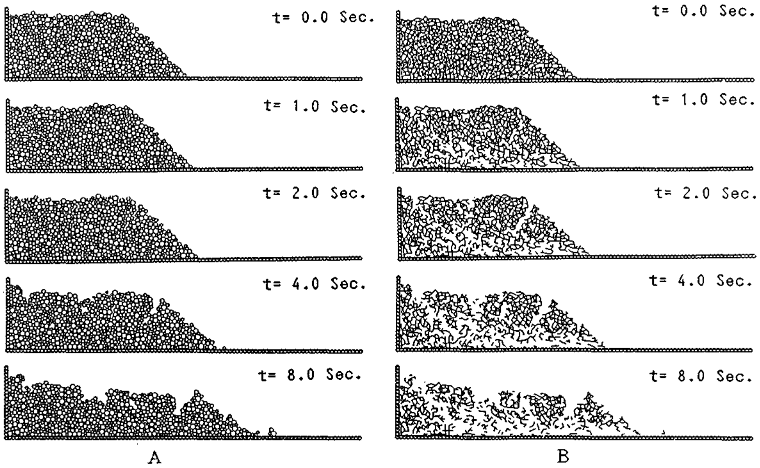

Fig. 12 Dynamics of Bank Collapse Caused by a Cyclic Loading (slope angle 45°).

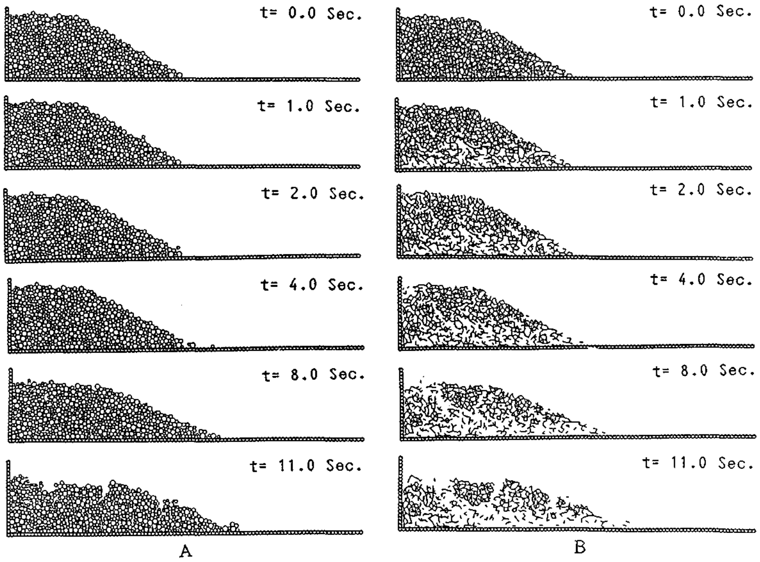

Fig. 13 Dynamics of Bank Collapse Caused by a Cyclic Loading (slope angle 30°).

The secondary structure can transmit the wave propagation. And it is destructible, then this system can represent the small cracks and the fracture process. It can detect crack and fracture lines and discriminate broken from stable areas, thereby extending the use of the DEM. The fracture process of the study is as follows ; Many small cracks occur in wide sphere, then some of them are connected and extend to the fracture lines. The stable area forms the clusters of soil and the secondary structures between two clusters are destroyed by the concentrated tensile force due to the relative movement betwen two clusters. This means that the modified DEM can be used to study problems of fracture in soils and soil structures that previously could not be investigated. And the secondary structure can transmit the wave propagation.

We think there is yet room for improvement in the method to decide the parameters and the fracture laws of the secondary structure.

We think the distinct element can be used in two cases. In one case, one distinct element corresponds to one particle as sand or rock. This method is suitable to study soil mechanics. In the other case, one element corresponds to one cluster or blocks of the medium as FEM. This method is suitable to study the micro-mechanics.

ACKNOWLEDGMENTS

All computations were made with the HITAC M 280 H computer at the Earthquake Prediction Center of the Earthquake Research Institute (ERI), the University of Tokyo. We thank Dr. K. Takano and Dr. K. Kohketsu (ERI) for their kind help with the computer and the use of their user-friendly program, ETERM.

REFERENCES

1) Cundall, P. A. : A Computer Model for Simulating Progressive, Large Scale Movement in Blocky Rock Systems, Symp. ISRM, Nancy, France, Proc. 2, pp. 129–136, 1971.

2) Hakuno, M. and Hirao, T. : A Trial Related to Random Packing of Particle Assemblies, Proc. Japan Society of Civil Engineering, Vol. 219, pp. 53–63, 1973.

3) Kiyama, H. Fujimura, H. and Nishimura, T. : Theoretical Analysis of Fenner-Pacher-Like Characteristic Curves for Tunneling by Distinct Element Method, Proc. Japan Society of Civil Engineering, Vol. 394, pp. 37–44, 1988.

4) Kiyama, H. and Fujimura, H. : Analysis on Gravity Flow of Rock Granular Assemblies by Cundall Model, Proc. Japan Society of Civil Engineering, Vol. 333, pp. 137–146, 1983.

5) Uemura, D. and Hakuno, M. : Granular Assembly Simulation with Cundall's Model for the Dynamic Collapse of the Structural Foundation, Proc. Japan Society of Civil Engineering, Vol. 380, pp. 181–190, 1987.

6) Casaverde, L., Iwashita, K., Tarumi, Y. and Hakuno, M. : Distinct Element Method for Rock Avalanche, Proc. Japan Society of Civil Engineering, Vol. 404, pp. 153–162, 1989.

7) Tarumi, Y. and Hakuno, M. : A Granular Assembly Simulation for the Seismic Liquefaction of Sand, Proc. Japan Society of Civil Engineering, Vol. 398, pp. 129-138, 1988.

(Received October 31 1988)